

PUBLISHED VERSION

Miftar Ganija, Nikita Simakov, Alexander Hemming, John Haub, Peter Veitch, and Jesper Munch

Efficient, low threshold, cryogenic Ho:YAG laser

Optics Express, 2016; 24(11):11569-11577

©2016 Optical Society of America

Published version <http://dx.doi.org/10.1364/OE.24.011569>

PERMISSIONS

Rights url: https://www.osapublishing.org/submit/review/copyright_permissions.cfm#

Creative Commons Licensing

OSA is aware that some authors, as a condition of their funding, must publish their work under a Creative Commons license. We therefore offer a CC BY license for authors who indicate that their work is funded by agencies that we have confirmed have this requirement. Authors must enter their funder(s) during the manuscript submission process. At that point, if appropriate, the CC BY license option will be available to select for an additional fee.

Any subsequent reuse or distribution of content licensed under CC BY must maintain attribution to the author(s) and the published article's title, journal citation, and DOI.

<http://creativecommons.org/licenses/by/4.0/>



This is a human-readable summary of (and not a substitute for) the [license](#).

[Disclaimer](#)



You are free to:

Share — copy and redistribute the material in any medium or format

Adapt — remix, transform, and build upon the material
for any purpose, even commercially.

The licensor cannot revoke these freedoms as long as you follow the license terms.

Under the following terms:



Attribution — You must give **appropriate credit**, provide a link to the license, and **indicate if changes were made**. You may do so in any reasonable manner, but not in any way that suggests the licensor endorses you or your use.

No additional restrictions — You may not apply legal terms or **technological measures** that legally restrict others from doing anything the license permits.

15 September 2016

<http://hdl.handle.net/2440/101197>

Efficient, low threshold, cryogenic Ho:YAG laser

Miftar Ganija,^{1,*} Nikita Simakov,² Alexander Hemming,² John Haub,² Peter Veitch,¹ and Jesper Munch¹

¹School of Physical Sciences and IPAS, The University of Adelaide, SA 5005, Australia

²Laser Technologies Group, Cyber and Electronic Warfare Division, DST Group, Edinburgh, SA 5111, Australia

*miftar.ganija@adelaide.edu.au

Abstract: We report the development of an efficient, liquid-nitrogen conduction cooled Ho:YAG slab laser with good beam quality. Detailed measurements resolving the structure of the 1900–1911 nm absorption band in Ho:YAG at 77 K are presented. Stress-free conduction cooled mounting of the Ho:YAG slab was demonstrated and the resulting laser operated with a large mode volume of 42 mm³, a slope efficiency of 75% and a threshold of 0.84 W. To our knowledge this corresponds to the lowest reported threshold intensity for a Ho:YAG laser.

©2016 Optical Society of America

OCIS codes: (140.3460) Lasers; (140.3510) Lasers, fiber.

References and links

1. D. Y. Shen, A. Abdolvand, L. J. Cooper, and W. A. Clarkson, "Efficient Ho:YAG laser pumped by a cladding-pumped tunable Tm:silica-fibre laser," *Appl. Phys. B* **79**(5), 559–561 (2004).
2. E. Lippert, S. Nicolas, G. Arisholm, K. Stenersen, and G. Rustad, "Midinfrared laser source with high power and beam quality," *Appl. Opt.* **45**(16), 3839–3845 (2006).
3. I. Elder, "Thulium fibre laser pumped mid-IR source," *Proc. SPIE* **7325**, 73250I (2009).
4. E. Lippert, H. Fonnum, G. Arisholm, and K. Stenersen, "A 22-watt mid-infrared optical parametric oscillator with V-shaped 3-mirror ring resonator," *Opt. Express* **18**(25), 26475–26483 (2010).
5. A. Hemming, J. Richards, A. Davidson, N. Carmody, S. Bennetts, N. Simakov, and J. Haub, "99 W mid-IR operation of a ZGP OPO at 25% duty cycle," *Opt. Express* **21**(8), 10062–10069 (2013).
6. S. Bennetts, A. Hemming, A. Davidson, and D. G. Lancaster, "110 W 790 nm pumped 1908 nm thulium fibre laser," in *Joint conference of the Opto-Electronics and Communications Conference and the Australian Conference on Optical Fibre Technology. OECC/ACOFT 2008*. (2008), p. 1–2.
7. D. J. Creeden, B. R. Johnson, and S. D. Setzler, "High Efficiency 1908 nm Tm-doped Fiber Laser Oscillator," in *Specialty Optical Fibers* (Optical Society of America, 2012), p. SW2F.4.
8. Y.-J. Shen, B.-Q. Yao, X.-M. Duan, G.-L. Zhu, W. Wang, Y.-L. Ju, and Y.-Z. Wang, "103 W in-band dual-end-pumped Ho:YAG laser," *Opt. Lett.* **37**(17), 3558–3560 (2012).
9. A. Hemming, J. Richards, S. Bennetts, A. Davidson, N. Carmody, P. Davies, L. Corena, and D. Lancaster, "A high power hybrid mid-IR laser source," *Opt. Commun.* **283**(20), 4041–4045 (2010).
10. J. I. Mackenzie, W. O. S. Bailey, J. W. Kim, L. Pearson, D. Y. Shen, Y. Yang, and W. A. Clarkson, "Tm: fiber laser in-band pumping a cryogenically-cooled Ho:YAG laser," *Proc. SPIE* **7193**, 71931H (2009).
11. J. I. Mackenzie, J. W. Kim, L. Pearson, W. O. S. Bailey, Y. Yang, and W. A. Clarkson, "Two-micron cryogenically-cooled solid-state lasers: recent progress and future prospects," *Proc. SPIE* **7578**, 75781F (2010).
12. P. H. Klein and W. J. Croft, "Thermal Conductivity, Diffusivity, and Expansion of Y₂O₃, Y₃Al₅O₁₂, and LaF₃ in the Range 77–300 K," *J. Appl. Phys.* **38**(4), 1603–1607 (1967).
13. G. A. Slack and D. W. Oliver, "Thermal Conductivity of Garnets and Phonon Scattering by Rare-Earth Ions," *Phys. Rev. B* **4**(2), 592–609 (1971).
14. R. Wynne, J. L. Daneu, and T. Y. Fan, "Thermal coefficients of the expansion and refractive index in YAG," *Appl. Opt.* **38**(15), 3282–3284 (1999).
15. D. C. Brown, J. M. Singley, E. Yager, K. Kowalewski, J. Guelzow, and J. W. Kuper, "Kilowatt class high-power CW Yb:YAG cryogenic laser," *Proc. SPIE* **6952**, 69520K (2008).
16. D. J. Ripin, J. R. Ochoa, R. L. Aggarwal, and T. Y. Fan, "165-W cryogenically cooled Yb:YAG laser," *Opt. Lett.* **29**(18), 2154–2156 (2004).
17. M. Ganija, D. Ottaway, P. Veitch, and J. Munch, "Cryogenic, high power, near diffraction limited, Yb:YAG slab laser," *Opt. Express* **21**(6), 6973–6978 (2013).
18. H. Fonnum, E. Lippert, and M. W. Haakestad, "550 mJ Q-switched cryogenic Ho:YLF oscillator pumped with a 100 W Tm: fiber laser," *Opt. Lett.* **38**(11), 1884–1886 (2013).
19. G. A. Newburgh, Z. Fleischman, and M. Dubinskii, "Highly efficient dual-wavelength laser operation of cryo-cooled resonantly (in-band) pumped Ho³⁺:YVO₄ laser," *Opt. Lett.* **37**(18), 3888–3890 (2012).

20. Z. D. Fleischman, L. D. Merkle, G. A. Newburgh, and M. Dubinskii, "Spectroscopic analysis of efficient laser material Ho³⁺:YVO₄," *Opt. Mater. Express* **3**(8), 1176–1186 (2013).
21. R. L. Aggarwal, D. J. Ripin, J. R. Ochoa, and T. Y. Fan, "Measurement of thermo-optic properties of Y₃Al₅O₁₂, Lu₃Al₅O₁₂, YAlO₃, LiYF₄, LiLuF₄, BaY₂F₈, KGd(WO₄)₂, and KY(WO₄)₂ laser crystals in the 80–300 K temperature range," *J. Appl. Phys.* **98**, 103514 (2005).
22. J. B. Gruber, M. E. Hills, M. D. Seltzer, S. B. Stevens, C. A. Morrison, G. A. Turner, and M. R. Kokta, "Energy levels and crystal quantum states of trivalent holmium in yttrium aluminum garnet," *J. Appl. Phys.* **69**(12), 8183–8204 (1991).
23. B. M. Walsh, G. W. Grew, and N. P. Barnes, "Energy levels and intensity parameters of Ho³⁺ ions in GdLiF₄, YLiF₄ and LuLiF₄," *J. Phys. Condens. Matter* **17**(48), 7643–7665 (2005).
24. E. Lippert, H. Fonnum, and K. Stenersen, "Fiber laser pumped high energy cryogenically cooled Ho:YLF laser," *Proc. SPIE* **8543**, 854308 (2012).
25. M. Ganija, D. J. Ottaway, P. J. Veitch, and J. Munch, "A Cryogenic, End Pumped, Zigzag Slab Laser Suitable For Power Scaling," in *Proceedings of the International Quantum Electronics Conference and Conference on Lasers and Electro-Optics Pacific Rim 2011* (Optical Society of America, Sydney, 2011), p. C817.
26. M. Ganija, D. J. Ottaway, P. J. Veitch, and J. Munch, "A Cryogenic, End Pumped, Zigzag Slab Laser Suitable For Power Scaling," in *Conference on Lasers and Electro-Optics/Pacific Rim* (Optical Society of America, 2011), p. C817.
27. P. E. Ciddor, "Refractive index of air: new equations for the visible and near infrared," *Appl. Opt.* **35**(9), 1566–1573 (1996).
28. N. Simakov, A. Hemming, A. Carter, K. Farley, A. Davidson, N. Carmody, J. M. O. Daniel, M. Hughes, L. Corena, D. Stepanov, and J. Haub, "170 W Single-mode Large Pedestal Thulium-doped Fibre Laser," in *2015 European Conference on Lasers and Electro-Optics - European Quantum Electronics Conference* (Optical Society of America, Munich, 2015), p. CJ_13_2.
29. N. Simakov, A. V. Hemming, A. Carter, K. Farley, A. Davidson, N. Carmody, M. Hughes, J. M. O. Daniel, L. Corena, D. Stepanov, and J. Haub, "Design and experimental demonstration of a large pedestal thulium-doped fibre," *Opt. Express* **23**(3), 3126–3133 (2015).

1. Introduction

High power and high energy 2.1 μm lasers with excellent beam quality are required for a wide range of industrial, scientific and defence applications. These lasers are useful in eye-safe remote sensing, laser radar, gravitational wave detection and as pump sources for optical parametric oscillators for the generation of mid-infrared radiation.

A potentially attractive laser host for operation in this wavelength region is holmium-doped yttrium aluminium garnet (Ho:YAG) which is typically pumped at 1908 nm and emits at 2090–2097 nm. This material has been investigated by many authors lasing at room temperature (RT) [1–5]. The laser is usually resonantly pumped around 1908 nm and takes advantage of a very small quantum defect (typically ~9%). Thulium fibre pump lasers at these wavelengths have been reported with powers of 100 – 200 W CW, enabling the potential scaling of Ho:YAG lasers and amplifiers in both power and pulse energy [6, 7].

However Ho:YAG is a quasi-3-level gain medium at room temperature and thus requires high intensity pumping to reach transparency. The resulting high lasing threshold intensities produce large thermal gradients, which degrade beam quality and risk laser crystal damage as the average output power is increased. The threshold powers per unit volume for RT Ho:YAG laser systems reported, vary from 0.3 W/mm³/wt.% [8] to 1.4 W/mm³/wt.% [4] with typical small mode diameters of about 0.5 mm. Our previous experiments have demonstrated a similar value of 1.1 W/mm³/wt.% [5, 9]. High peak power operation and pulse energy scaling of Ho:YAG lasers, enabling their use as sources for long wavelength frequency conversion, will require substantially larger mode areas in order to avoid catastrophic optical damage.

It has previously been demonstrated that cryogenic cooling of the laser gain medium can address the problems associated with the 3-level nature of Ho:YAG [10, 11]. Cooling the gain medium to cryogenic temperatures (CTs), redistributes the thermal population of the ground state manifold, resulting in 4-level laser behavior. This substantially reduces the pump intensity required to achieve transparency and reach laser threshold. Furthermore, operating at CTs dramatically increases the thermal conductivity and decreases both the thermal expansion coefficient and dn/dT in the crystalline YAG host [12–14]. Several liquid nitrogen (LN) cooled Yb:YAG lasers have demonstrated these advantages with high average power and good beam quality using disk [15], rod [16] and slab [17] gain media. However these thermo-opto-mechanical properties have yet to be exploited in Ho:YAG. Substituting Ho³⁺

doping for the Yb^{3+} doping thus appears to be a simple and promising approach to achieving these advantages at longer wavelengths.

A similar approach has been demonstrated in Ho:YLF at 2050 nm and scaled to an impressive 550 mJ pulse energy [18]. A LN cooled Ho:YVO₄ laser has also been reported by Newburgh *et al.* with excellent efficiency [19] and a comprehensive cryogenic spectroscopic characterization has also been undertaken for Ho³⁺ in this host [20]. Both YLF and YVO₄ are birefringent materials however, and while offering similar thermo-optic and thermo-mechanical advantages at CTs [21] Ho³⁺ ions in these hosts lase at shorter wavelengths and are less suited for the desired applications. In contrast Ho:YAG is an isotropic material and as a result does not require a linearly polarized pump source, or a double pass pumping configuration. This greatly simplifies the construction of the thulium fibre pump laser and the optical arrangement for delivering the pump beam to the gain medium. The longer operating wavelength of Ho:YAG is also advantageous when pumping materials such as Zinc Germanium Phosphide. Thus resonantly pumped, cryogenic Ho:YAG, lasing at 2 μm appears to be an attractive approach to enable peak and average power scaling of sources operating at wavelength ~ 2100 nm.

Previous authors [22, 23], have shown that the nature of Stark splitting in Ho³⁺ in YAG on each manifold is complex with a multitude of transition lines. As a result the corresponding absorption spectrum of the ⁵I₈ manifold is broad and consists of many features [22, 23]. Mackenzie *et al* [10] reported a LN cooled Ho:YAG laser pumped by a thulium-doped fibre laser (TDFL) at 1932 nm that produced about 8 W of output power with a slope efficiency of 28%. The authors also described substantial narrowing of the pump absorption in the Ho:YAG as they reached CTs. Such narrowing has also been observed in Ho³⁺ in YLF and YVO₄ [18, 20, 24]. Our work seeks to address some of the issues raised by this preliminary Ho:YAG lasing demonstration and spectroscopic investigation, and demonstrate an approach for developing an efficient, cryogenic Ho:YAG laser.

While cryogenic cooling offers significant advantages, it also presents substantial challenges. A successful cryogenic laser must utilize a mechanical design that allows for maximum conduction cooling and minimum stress-induced wave-front distortions and birefringence when pumped and lasing at CT's. The design must permit assembly at RT and have the ability to allow repeated cryogenic cooling cycles. The design also needs to be based on the choice of low rare-earth doping concentrations to maximize the thermal conductivity of the laser material [13], thereby allowing the full advantages of the thermo-optical properties of YAG at CTs to be exploited.

In this paper we present the absorption spectra of Ho:YAG, including high resolution measurements in the 1900 - 1911 nm spectral region at 77 K. We demonstrate the validity of our approach with a preliminary demonstration of a conduction cooled cryogenic Ho:YAG laser and achieve a low threshold corresponding to <0.03 W/mm³/wt.%. This demonstrates a reduction in threshold intensity by more than an order of magnitude, compared to the RT operation of Ho:YAG. By matching the pump laser emission to the measured narrow absorption features, we achieve a slope efficiency of 75%. These results represent a substantial contribution to the development of cryogenic Ho:YAG lasers.

Note on temperatures: in the case of spectroscopic results we quote the temperature of the laboratory (~ 295 K) and that of liquid nitrogen (77 K). For pumped laser material we use room temperature (RT) and liquid nitrogen (LN) cooled to indicate that the precise temperatures of the materials were not measured but are known to be slightly higher than 295 K and 77 K respectively.

2. Ho:YAG absorption spectrum around 1908 nm

Measurements of the absorption spectrum of the Ho:YAG crystal were performed by using a super-continuum source (SuperK, NKT Photonics) and an optical spectrum analyser (OSA) (Yokogawa AQ6375) as shown in Fig. 1. A Ho:YAG slab with a nominal Ho³⁺ doping concentration of 0.7 wt.% and length 49 mm was characterised.

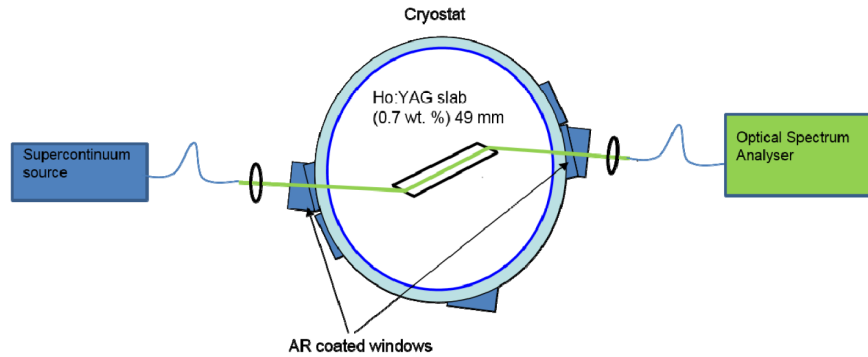


Fig. 1. Schematic of the experimental setup for the measurement of the transmission through the Ho:YAG crystal at 295 K and 77 K.

The absorption spectra obtained over a broad wavelength range are shown in Fig. 2. These spectra clearly demonstrate the complexity of the transitions from the 5I_8 manifold to the ground state. Also evident is the suppression of the quasi-3 level reabsorption losses around 2000-2100 nm when the sample is cooled from 295 K to 77 K, thus confirming the transition to the 4-level laser behavior of Ho:YAG at CTs.

Detailed measurements of the absorption spectra in the 1900-1911 nm region are shown in Fig. 3. This spectral region corresponds to that typically used to pump Ho:YAG at RT due to the strong, broad absorption feature around 1907 nm. It was observed that the absorption coefficient at 1908.3 nm increased from $\sim 1 \text{ cm}^{-1}$ to $\sim 1.8 \text{ cm}^{-1}$, and narrowed significantly as the temperature was lowered from 295 K to 77 K.

To allow background data subtraction of the absorption measurement, the atmospheric absorption data was recorded using the identical experimental setup, but with the Ho:YAG sample removed. The known water lines were observed as shown and their wavelengths were used to ensure the calibration of the OSA.

In further experiments, tuning of the pump laser wavelength allowed us to validate these absorption measurements as shown in the inset of Fig. 3. The figure shows the Ho:YAG laser output power as a function of pump wavelength over the range 1906.8 – 1908.3 nm where the pump laser could be reliably tuned. Operation at both absorption peaks yielded similar efficiencies and thresholds and pumping at 1908.3 nm was chosen for further laser development.

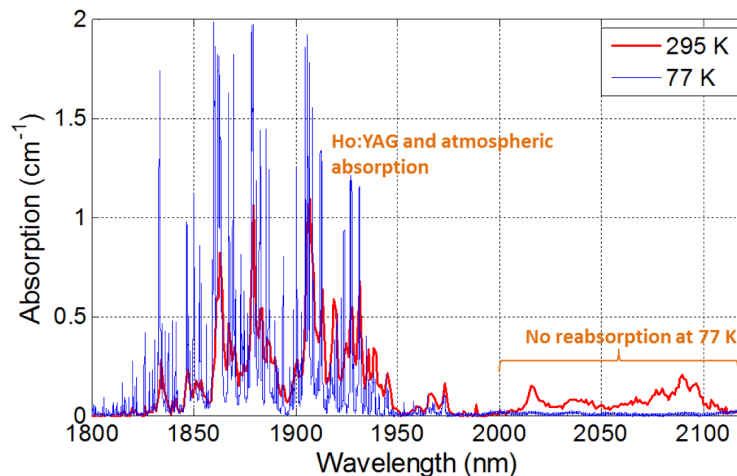


Fig. 2. The absorption spectra of a 0.7 wt% doped Ho:YAG laser slab at 295 K and 77 K. These measurements were made with an OSA resolution of 0.5 nm.

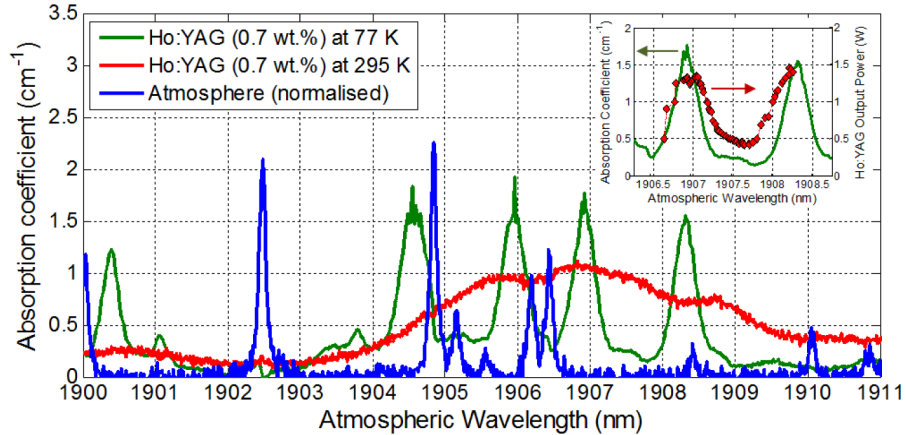


Fig. 3. Absorption spectra of 0.7 wt% doped Ho:YAG at 295 K (red) and at 77 K (green) with the atmospheric absorption superimposed (blue). These measurements were made with a verified OSA resolution of 0.1 nm. Inset: Ho:YAG absorption spectrum at 77 K superimposed with preliminary laser results in which tuning of the pump wavelength across the absorption features was demonstrated to result in a variation in absorbed pump power and hence Ho:YAG output power.

3. Cryogenic laser

3.1 Mounting of the laser crystal

A key design criterion for cryogenic laser operation is the minimization of the applied stress that could lead to wave-front distortion and induced birefringence from differential thermal contraction when the laser gain medium is cooled to 77 K. In this work the mechanical laser head architecture is similar to that described elsewhere [17, 25] and uses an indium-molybdenum-aluminium design to maximize thermal conductivity to the cold finger, while minimising the mechanical stress applied to the laser crystal. The laser crystal used was a 2 mm thick, 3 mm wide, 49 mm long 0.7% wt. Ho:YAG slab with end faces cut at Brewster's angle.

To mount the laser slab we followed the approach described in [17] and [26]. To ensure optimal stress-free mechanical mounting the slab was monitored interferometrically (with a 632.8 nm HeNe laser) at RT and when cooled to 77 K. The resulting interferograms are shown in Fig. 4. These measurements were performed without pumping the laser slab and are thus measures of the cryo-mechanical stress only. The compact resonator and the bulk of the cryostat prevented us from making interferometric studies while lasing. However such measurements have been performed previously for a similarly mounted Yb:YAG slab [17] where no pump-induced stress was observed at thermal loads much larger than those reported here. These observations are ascribed to the significantly improved thermo-optic properties of YAG at cryogenic temperatures. While it can be seen that the slab is not of perfect optical quality, due to the presence of slightly curved fringes, the important aspect of the interferograms is the lack of the appearance of any additional stress when the slab was LN cooled.

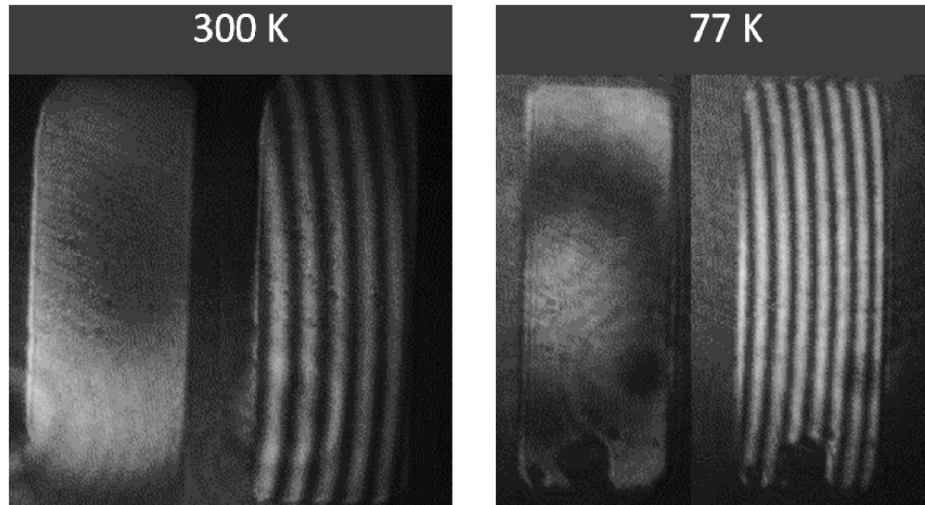


Fig. 4. Interferograms of the unpumped Ho:YAG gain medium at 300 K and when cooled to 77 K, demonstrating no new distortions from the cooling and mechanical mount. Shown for both cases are the zero-fringe and carrier-fringe alignment recorded using a 'straight through' probe beam. The wavelength used for the interferometry was 632.8 nm. The artefact at the base of the crystal is a damaged region observed after multiple assemblies.

3.2 Laser design

The optical layout of the laser designed with straight through axes of both pump and lasing beams is shown in Fig. 5, including the vacuum envelope of the cryostat, the windows through which the pump (green) and laser beam (red) pass and the laser resonator formed by mirrors M2 and M3.

The pump source was an un-polarized tunable thulium-doped fiber laser with narrow emission bandwidth (<0.1 nm) and excellent wavelength stability (<0.05 nm). The pump laser provided an output with diffraction limited beam quality (M^2 of <1.05) and excellent pointing stability under all operating conditions. The output wavelength of the pump laser could be tuned by controlling the temperature of the fibre Bragg gratings in the laser.

The 1908 nm pump beam was collimated by an aplanatic lens ($f = 25$ mm) and launched into the laser crystal via a dichroic mirror, D1 (high transmission (HT) at 1908 nm and high reflectivity (HR) at 2097 nm). A polarizing beam splitter was used to separate the p and s polarisations of the pump. This allows the Ho:YAG crystal to be pumped by the p-polarisation avoiding pump reflection at the Brewster angled surfaces of the Ho:YAG crystal. The optical loss of each cryostat window was measured to be 1.5% at both the pump and laser output.

The Fresnel reflection from an uncoated CaF_2 wedge at near normal incidence was used to monitor the pump power launched into the Ho:YAG crystal. The use of the monitoring wedge ensured that any polarization or power fluctuations of the pump laser did not affect the subsequent power and slope efficiency measurements.

The resonator mirrors (M2 and M3) were both concave with nominal radii of curvature of 500 mm and separated by 800 mm. At 2097 nm, M2 is HR and M3 has a reflectivity of 70%.

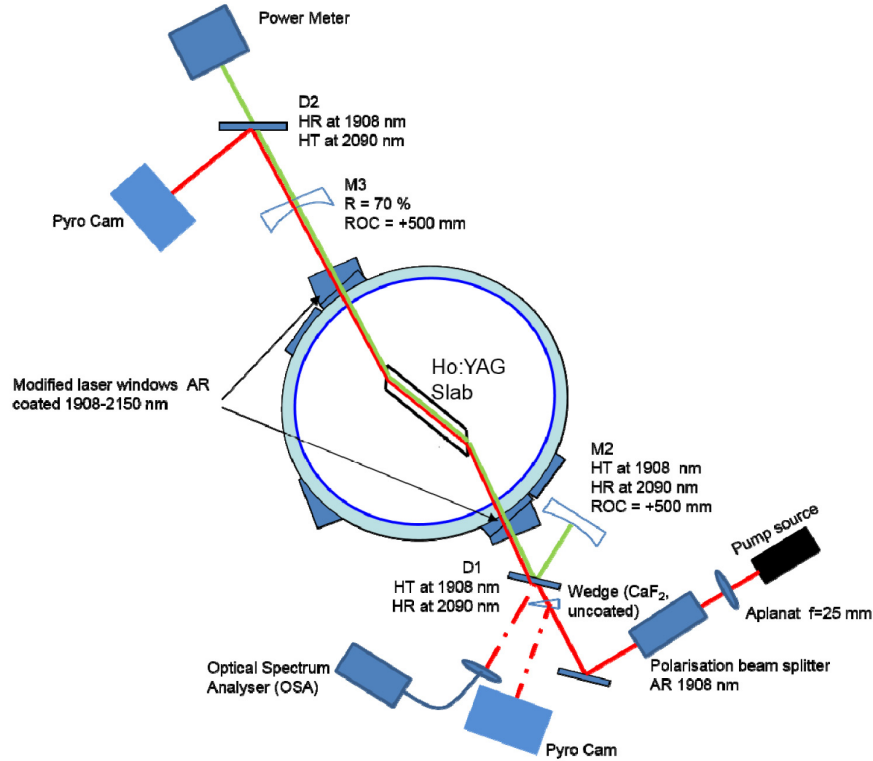


Fig. 5. Schematic of the optical layout of the laser in the cryostat as described in the text, including the external pump laser optics and the diagnostics used.

4. Cryogenic Ho:YAG laser results

The output power is shown in Fig. 6 as a function of launched pump power. The pump absorption was >99% due to the combination of the strong absorption cross-section at this wavelength, the narrow linewidth of the pump laser and the crystal length. The threshold was measured to be 0.84 W and the laser operated with a slope efficiency of 75%.

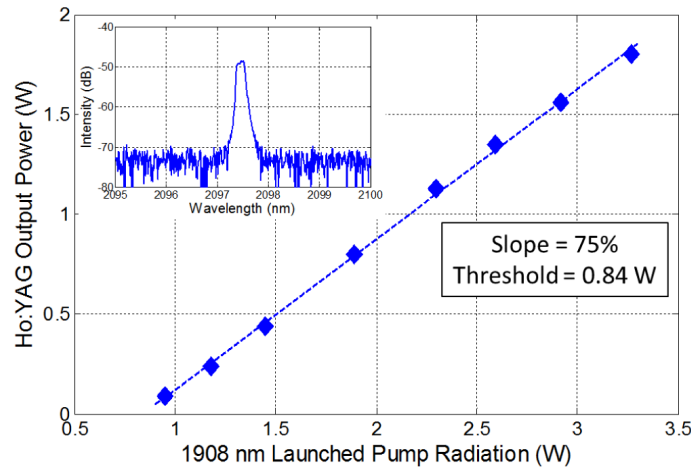


Fig. 6. Output power, slope efficiency and spectral content of the LN cooled Ho:YAG laser.

The dimensions of the pump and laser modes at the center of the laser crystal were measured using an imaging system. The sagittal $1/e^2$ mode diameter of the pump and lasing modes were measured to be 0.77 mm and 0.7 mm respectively. Due to the Brewster angle cut surface, the pump and laser mode dimensions inside the slab were anamorphic at 1.40 mm x 0.77 mm and 1.27 mm x 0.7 mm. The laser mode dimensions were consistent with that predicted by an ABCD model of the resonator.

The beam quality of the output was determined by focusing the output beam and measuring the beam size near the waist. An imaging system with a magnification of 5.0 was used to ensure accurate measurements of the beam diameter near the waist. The corresponding measured diameters, curves of best fit and images of the near field and far field profiles are shown in Figs. 7(a)–7(c). The imperfect beam quality was attributed in part to the low quality of the laser slab surfaces (Fig. 4) and in part to the residual clipping of the beam as we were aiming to maximize the volume of the slab that we were pumping/lasing in.

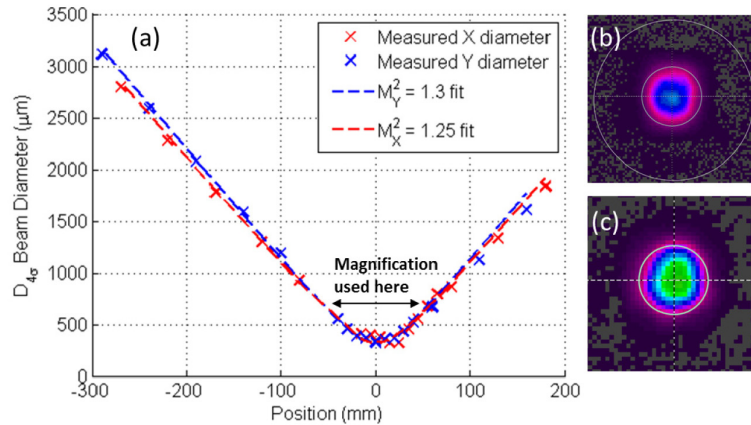


Fig. 7. (a) Waist diameter measurements and fit lines resulting in an $M^2_{X,Y} = 1.3, 1.25$. (b) Near field profile of the Ho:YAG output. (c) Far field profile viewed with an imaging system with a magnification of 5.0.

5. Discussion

The absorption of Ho:YAG was characterized at 295 K and 77 K. As previously reported, the reabsorption in the 2000–2100 nm wavelength range was suppressed with cooling, resulting in the crystal effectively becoming a 4-level system. We also report the narrowing of the 1908 nm absorption band and its splitting into four distinct peaks. Preliminary investigation by the tuning of the thulium pump laser confirmed the presence of these absorption features. Figure 3 also shows an overlay of the atmospheric absorption which enables the selection of pump wavelengths that can propagate without atmospheric attenuation over distances that would be typically relevant in a laboratory environment.

These measurements allowed us to identify the specific electronic transitions in this spectral region. Using a calculated refractive index of air at 1908 nm of ~ 1.000273 [27], the wavenumbers of the peaks of the four absorption lines were found to be 5239, 5243, 5245 and 5249 cm^{-1} , which agreed with those published by Gruber et al [22]. For example the 1908.3 nm absorption line used in this work corresponds to 5239 cm^{-1} and thus the Z_2 to Y_3 transition.

It should be pointed out the 1.8 cm^{-1} feature in Fig. 3 is at the limit of the dynamic range (40 dB) of our measurement system. It is also possible that the measurement is limited by the resolution utilised (0.1 nm) and the strength of the absorption features. In order to resolve the specific features more accurately, it is recommended that a tuneable single frequency source and a shorter crystal length is utilised. This would allow for a very narrow resolution measurement with a much larger dynamic range.

Bearing in mind the limitations of our preliminary measurements, the spectral width of these transitions appears to be about 0.3 nm, which compares favourably with the < 0.15 nm line width of high power (> 100 W) thulium fiber lasers operating in this wavelength region [28, 29]. Thus, it would appear that such pump sources are suited to the future power scaling of cryogenic Ho:YAG lasers.

Using our previously developed mounting technique, we demonstrated low-stress mounting of a LN-cooled Ho:YAG laser slab. A laser cavity was constructed around the LN cooled gain medium and the laser operated with a threshold of 0.84 W and a 75% slope efficiency up to a maximum power of 1.75 W. This represents a threshold of <0.03 W/mm³/wt.%, a reduction by more than an order of magnitude in comparison to RT operation. These results show great promise for further power and energy of Ho:YAG lasers.

6. Conclusion

We have described the first LN cooled Ho:YAG laser pumped using the Z₂ to Y₃ transition, at a wavelength of 1908.3 nm. The threshold pump power density was lower by more than an order of magnitude in comparison to RT operation. The laser performance represents the lowest threshold power (0.84 W) and highest slope efficiency (75%) for a cryogenic Ho:YAG laser yet reported.

The Ho:YAG slab was mounted with a laser head designed to minimize wavefront distortion due to differential thermal contraction during LN cooling, and the laser operated with a good beam quality, consistent with the laser crystal and design used.

Future work will focus on scaling this approach to higher average power and investigation of pulsed operation.

Acknowledgment

The authors gratefully acknowledge support from the DST-Group and IPAS pilot project and excellent support from the Physics workshop at the University of Adelaide.